

An Infrared Test Camera for LBT adaptive optics commissioning

Italo Foppiani^{*a}, Matteo Lombini^b, Giovanni Bregoli^b, Giuseppe Cosentino^a, Emiliano Diolaiti^b,
Giancarlo Innocenti^b, Daniel Meschke^c, Ralf-Rainer Rohloff^c, Thomas M. Herbst^c,
Costantino Ciattaglia^b.

^aUniversità di Bologna – Dipartimento di Astronomia, via Ranzani 1, 40127 Bologna, Italy;

^bINAF – Osservatorio Astronomico di Bologna, via Ranzani 1, 40127 Bologna, Italy;

^cMax-Planck-Institut für Astronomie, Königstuhl 17, D-69117 Heidelberg, Germany.

ABSTRACT

A joint project among INAF – Osservatorio Astronomico di Bologna (Italy), Università di Bologna – Dipartimento di Astronomia (Italy) and Max-Planck-Institut für Astronomie (Heidelberg, Germany) led in about one year to the construction of two infrared test cameras for the LBT Observatory. Such cameras will be used to test the performance achieved by the telescope adaptive optics system as well as to prepare the telescope pointing model and to completely test all the focal stations at the Gregorian focus.

In the present article the design and the integration of the two test cameras are described. The achieved performances are presented as well.

Keywords: LBT, Large Binocular Telescope, infrared imaging, adaptive optics, commissioning.

1. INTRODUCTION

In October 2006 the LBT Observatory invited the LBT partners to submit a proposal for the construction of two InfraRed (IR) Test Cameras (TCs) dedicated to the commissioning of the forthcoming Adaptive Optics (AO) system of the Large Binocular Telescope [1] based on the adaptive secondary mirrors [2].

The main requirement of the TCs was the acquisition at high frame rate, 100 Hz or more, of diffraction limited images at infrared wavelength in order to measure the correction achieved by the AO system on both laboratory and on sky tests. The TC number one would have been dedicated to laboratory test at INAF Astrophysical Observatory of Arcetri (Florence, Italy) while the number two, identical to the first, would have been dedicated to on sky tests at the LBT. This camera would have been the first instrument installed at the telescope Gregorian focus so it would have been used to prepare the telescope pointing model and to carry out a complete commissioning of the Gregorian focal stations. A delivery time as short as one year was required not to delay the telescope commissioning and the AO development. Finally a careful evaluation and trade off between performance and cost were requested as well.

In December 2006 our joint proposal was selected and after a detailed review of the requirements we had the kick-off meeting in March 2007. In January 2008 we delivered the first IR TC in Arcetri and in April 2008 we successfully delivered the second unit on the mountain.

Commercial components have been used as much as possible because of the very tight time schedule of the project and in order to reduce the total cost. For instance the imaging device was chosen among commercially available IR cameras because it would have been impossible to develop it in less than one year and the cost would have been too high for the purpose of the instrument. Moreover commercial cameras commonly show the frame rate performance required.

The optical system has been based on a custom lenses design not only to meet the high resolution performance required but also to provide different configurations with different Fields of View (FoVs). The 3" FoV achievable with a proper sampling of the diffraction limited PSF (10mas/pixel) was indeed too narrow to allow to point any object on sky especially without any telescope pointing model since it would have been prepared by means of the TC itself. A wide FoV configuration (30") was thus implemented to easily point the TC and to acquire intra-focal and extra-focal images

* italo.foppiani@unibo.it; phone +39-051-2095706; fax +39-051-2095700

needed to refine the telescope collimation table. A third FoV of 6", just double than the narrow one, was also implemented to measure the wings of the diffraction limited PSF.

The different optical configurations are obtained repositioning two lenses which are mounted on motorized linear stages. Two more motorized units allow to position the optical filters (J or H) and the pupil stops on the optical path. All the positioners are remotely controlled to easily change the system configuration without the need to directly access the instrument.

Finally a liquid cooling system was implemented to chill all the heat dissipating surfaces in order to not introduce any air turbulence especially in the critical regions inside the TC and in front of the AO wavefront sensor.

2. DESIGN

2.1 Optical design

The optical system and imaging camera have been the key components around which the TCs have been designed. The pixels scale and the dimensions of the detector gave the constraints for the optics which fixed the requirements for the mechanics and the electronics.

Since the radius of the diffraction limited PSF of one single primary mirror of the telescope is about 30mas at 1 μ m wavelength, a sampling of about 10mas per pixel was required to properly model the AO corrected PSF. With such scale the available detector sizes of 320 \times 256 pixels or 640 \times 512 pixels would have given FoVs of 3.2" \times 2.6" or 6.4" \times 5.1". Since the TC would have been the very first instrument installed at the Gregorian focus and since up to that moment the telescope would have been operated with a 30' FoV imager at the prime focus (LBC [3]), it would have been very difficult to point any target on sky with such narrow FoVs especially without any pointing model. Moreover they would have been too narrow also to acquire the intra-focal and extra-focal images required to refine the telescope collimation table by means of curvature sensing techniques. A pixel scale of 100mas per pixel was thus judged mandatory to easily point the TC as well as to prepare the telescope pointing model and the collimation table during the Gregorian focus commissioning.

Different optical schemes providing the two pixel scales were investigated paying attention to their performance with respect to the final cost of the instrument. The eventual scheme was based on three calcium fluoride lenses two of which were repositionable in order to change the pixel scale on the detector. Moreover the lenses were optimized also for a third scale of 20 mas per pixel well suited to measure the wings of the AO corrected PSF by means of a 320 \times 256 pixels detector. In this way were able to cover the FoV need to measure the PSF wings by means of a camera with a small detector whose cost, about 30K€, was roughly one half of a camera with a 640 \times 512 pixels detector.

The eventual detector was thus an array of 320 \times 256 pixels with 30 μ m pitch which gave 3.2" \times 2.6", 6.4" \times 5.2" and 32" \times 26" FoVs at the different scales of 10, 20 and 100 mas per pixel. In figure 1 the lenses positions are sketched for the three optical configurations.

The entrance window of the TC is a dichroic, not shown in figure 1, which reflects the visible light toward the AO WFS and transmit the infrared light inside the TC. The AO WFS is located inside the AGW unit (Acquisition, Guiding and Wavefront sensing [4]) which provides the mechanical interface to which the TC is mounted and to which the scientific instrument will be attached. The entrance dichroic of the TC is identical and in the same position as the dichroic of the forthcoming scientific instrument (LUCIFER [5]).

As shows in figure 1 the lens number 1 (L1) is very close to telescope focal plane and remains fixed in all configurations while the lenses number 2 and 3 (L2 and L3) are repositioned along the optical axis. The total length of the system from the dichroic, located about 180mm before L1, to the image plane is constant and it is about 300mm. The lenses L2 and L3 are repositioned by means of two linear stages of 200mm travel. This scheme has the advantage to be easily adjustable at any time: for instance the lenses positions are refined depending on the filters selected in order to always deliver the best optical quality. Moreover L2 and L3 can be repositioned to obtain the out of focus images needed for curvature sensing instead of moving the telescope secondary mirror. Finally the lenses can be easily adjusted to deal with any possible coarse misalignment. This could have been useful especially during the first installation in the laboratory or at the telescope.

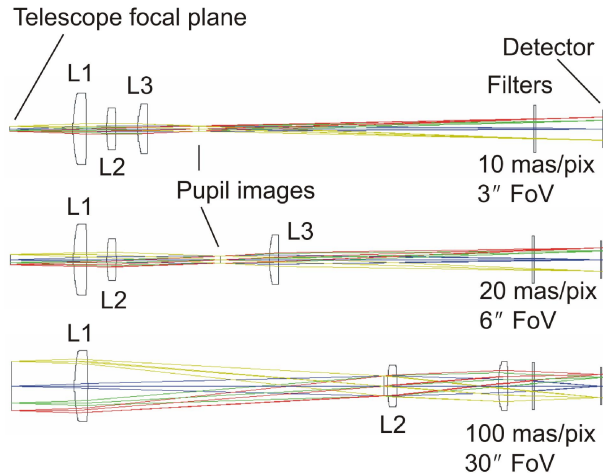


Figure 1 Sketch of the different optical configuration achieved translating the lenses L2 and L3 along the optical axis.

The tolerances on centring and on axial positioning of the lenses are about $\pm 0.1\text{mm}$ while for the tip tilt are about $\pm 5\text{mrad}$. These constraints are easily fulfilled by the standard linear stages used to reposition the lenses.

Two optical filters can be inserted just in front of the image plan (figure 1) by means of a dedicated positioner. The first filter is a custom filter by Omega Optical realized combining the standard narrow band pass filter 1075AF50 with an extended IR blocker to attenuate the out-of-band transmission to 10^{-5} . The resulting filter is a narrow blue version of the J filter with a central wavelength of $1.075\ \mu\text{m}$ and a full width half maximum (FWHM) of about $50\ \text{nm}$. The second filter, JDSU catalogue number W01661-13H, is similar to a H filter with a central wavelength of $1.65\ \mu\text{m}$ and a FWHM of about $300\ \text{nm}$ but its band pass is affected by the detector cut off at $1.7\ \mu\text{m}$ (figure 7). Its out-of-band transmission is about 10^{-3} .

The K band has not been implemented because it would have required a complete cryogenic system whose cost would have been too high for the purpose of the project.

In table 1 the nominal performance of the optical system for the different configurations are summarized. For the medium and narrow FoVs the figure of merit is the wavefront error and its related Strehl ratio (SR) as they have been designed to acquire diffraction limited images. The intrinsic values of SR are high enough to not affect the measurement of the AO performance. For the wide FoV the enclosed energy (EE) is considered as figure of merit because it has been designed to acquire seeing limited images.

Configuration	Image quality	
	1075AF50 filter (J)	W01661-13H filter (H)
10 mas/pixel	On axis WFE 30 nm (SR 0.97)	On axis WFE 42 nm (SR 0.97)
20 mas/pixel	On axis WFE 27 nm (SR 0.98)	On axis WFE 48 nm (SR 0.96)
100 mas/pixel	80% EE in $\sim 2 \times 2$ pixel	80% EE in $\sim 2 \times 2$ pixel

Table 1 Summary of image quality. WFE: polychromatic wavefront error subtracting the piston and tilt. SR: Strehl Ratio. EE: ensquared energy.

In figure 1 are visible the positions of the pupil images for the different configurations. A dedicated positioner inserts the proper stops around the pupil images for the narrow and the medium FoVs. The stop for the wide FoV is permanently mounted on the L2 mount since it is big enough not to affect the other configurations.

2.2 Mechanical design

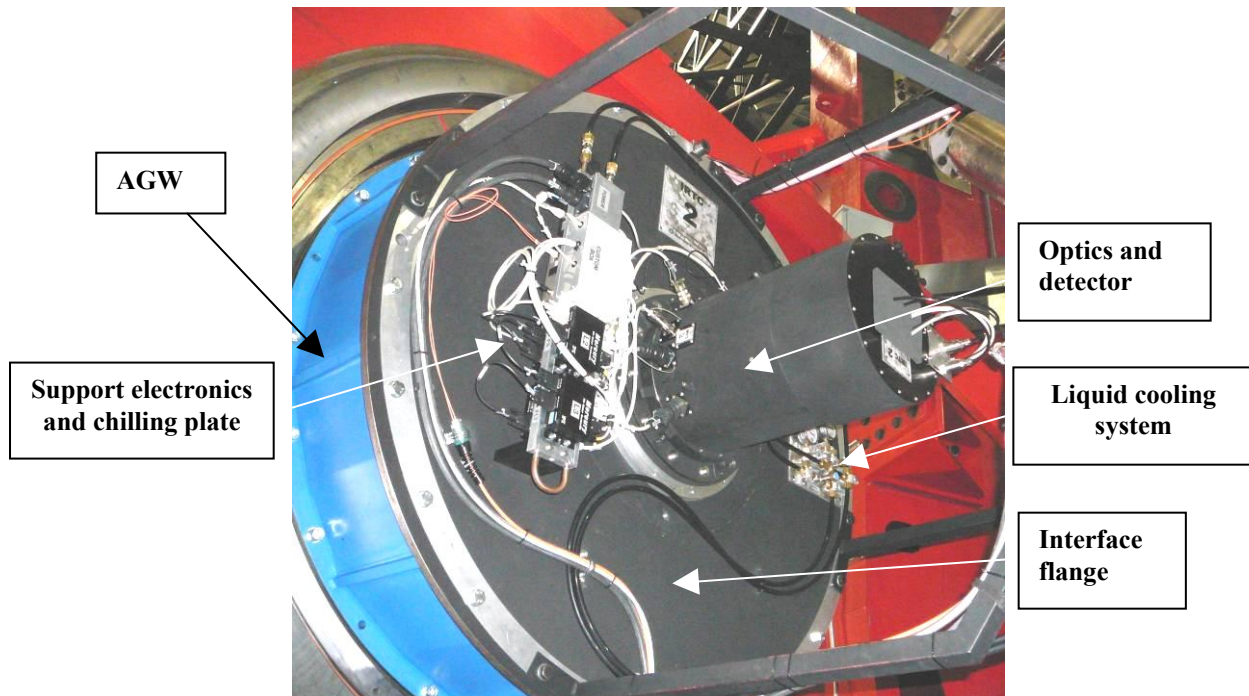


Figure 2 View of the TC number 2 installed on one of the LBT Gregorian focal station.

Figure 2 shows the TC installed at one of the focal stations at the bent Gregorian focus of the telescope. The mechanical components of the TC are basically two: the 1.5m diameter flange, which is the interface to the AGW unit, and the central cylinder where optics and detector are located in. The interface flange, made in aluminium, is 40mm thick to guaranty a flexure below 2 mas per degree change in elevation for either installations at the straight or bent Gregorian focal stations where the gravity vector is orthogonal or coplanar with respect to the flange. Moreover the TC can be rotated over 360° by the focal station derotator. In figure 3 the finite element analysis of the flange is shows for different angles.

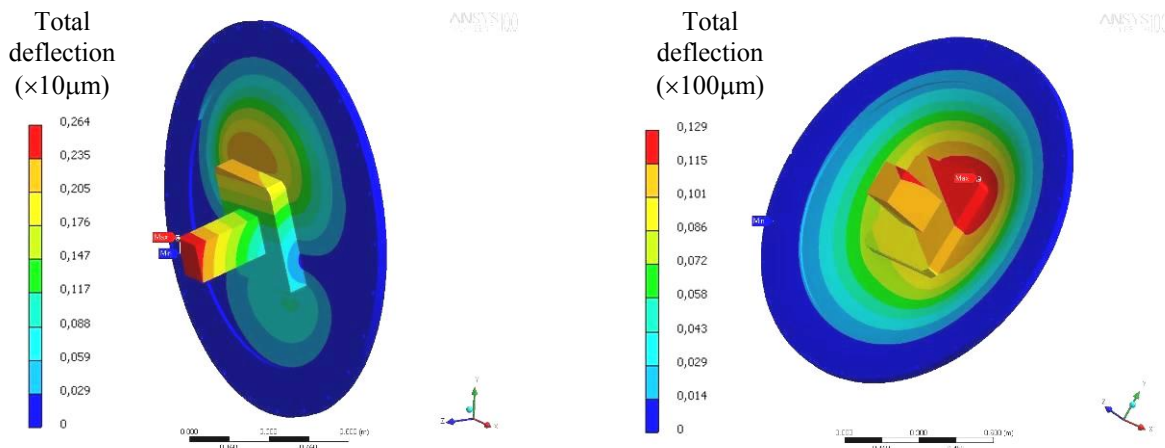


Figure 3 Finite element analysis of the 1.5m diameter flange. The flange is bounded at the edge and the weight of the rest of system is applied at the centre. The left image refers to the gravity vector parallel to the flange plane and right one refers to the gravity vector tilted by 45°.

The central part of the interface flange (the inner flange) can be detached from the outer part (outer flange) to easily handle the optical system during the alignments in the laboratory. The dichroic window is mounted at the centre of the

inner flange while the rest of the optics are mounted on the central cylinder. This cylinder is actually a semi-cylindrical support structure with two covers: one semi-cylindrical above and one cylindrical on one side. The lenses and the IR camera are mounted on this support which is attached to the inner flange by means of a mechanical interface that allows an adjustment of $\pm 5\text{mm}$ for centring and tip-tilting. An engineering view of the support structure with the lenses mounts and the motorized positioners is shown in figure 4. The two motorized units with the filters and the pupils stops are well visible between the two linear stages 200mm long. The L1 mount is visible on one side of the support structure while the IR camera is mounted at the opposite side.

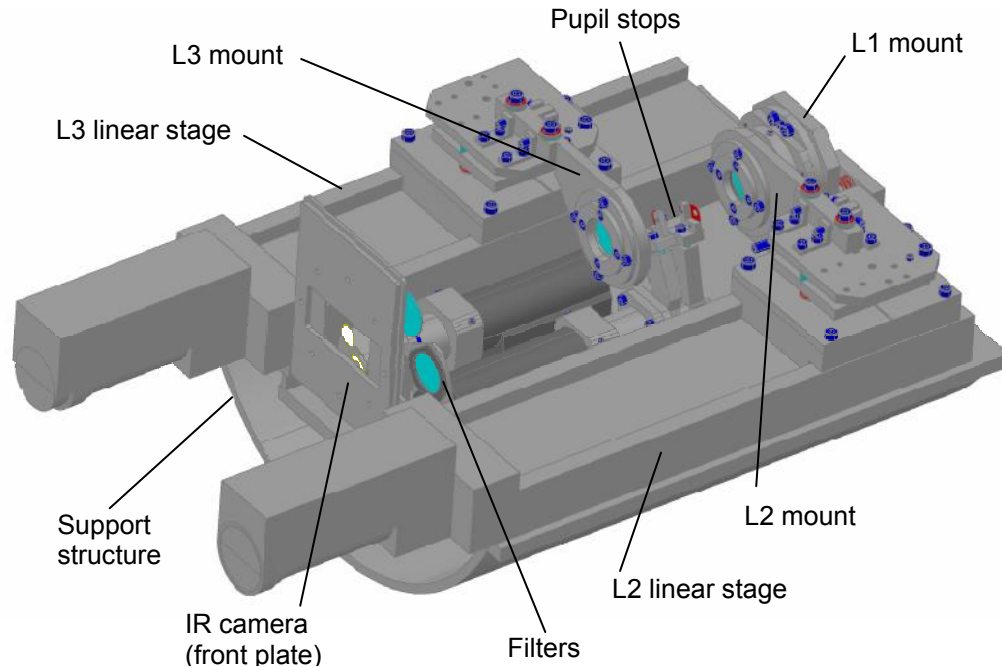


Figure 4 Engineering view of the support structure with the lenses mounts and the motorized positioners. Just the front plate of the IR camera housing is down to show the camera position. The detector is centred on the hole and coplanar with the plate.

The linear stages and the motors of the pupil stops and filters units are commercial components supplied by Physik Instrumente[†] (PI) while the remaining mechanics has been realized on a custom design.

The linear stages model is M-403.8DG with DC motor and gear box. Its performance, in term of carriage wobbling and positioning repeatability, are about ten times better than the required by the optical tolerances. The motor model used for the filters and pupil stops units is the C-136K018 with a modified gear ratio of 161:1 to increase the positioning repeatability. A photoelectric sensor has been used as position reference on the pupil stops units to reach the required absolute repeatability of $50\mu\text{m}$.

Finally a liquid cooling system has been implemented to chill all the heat dissipating surfaces in order not to induce any air turbulence in the ambient around the TC and in the very delicate regions inside the TC and in front of the AO wavefront sensor. A distribution system, visible in figure 2, allows to separately control the liquid flux through the chilling plate of the support electronics and through the IR camera.

2.3 Electronic and software design

The IR camera, which is a core component of the TC, has been selected among commercially available cameras because the development of a custom system would have been too expensive for the technical purpose of the instrument and it would have required a long time period not compatible with the schedule of the project. Moreover the frame rate and the dynamic range required were basically fulfilled by standard cameras.

[†] Physik Instrumente (PI) GmbH & Co. KG, Auf der Römerstrasse 1, D-76228 Karlsruhe/Palmbach, GERMANY

The spectral region covered by the camera was the first crucial parameter investigated. Different detector technologies, as mercury-cadmium-telluride and indium-antimonide have been taken into account but they required a deep cooling to control the dark current and they were quite expensive. Moreover considering the impact of a full cryogenic design to cover the K band, we decided not to cover this band to reduce the cost of the system simplifying its design and making use of a indium-gallium-arsenide (InGaAs) detector. This kind of detector covers only the spectral region from 0.9 μm to 1.8 μm but it does not require deep cooling and it is less expensive than other technologies (about 40% less).

Taking into account the working temperature constrains from -15 $^{\circ}\text{C}$ to +25 $^{\circ}\text{C}$ and the detector format, the two cameras available on the market were the Xeva XFPA-1.7 by XenICs[‡] and the SC4000 by FLIR[§]. Even if the detectors performance were comparable, the former was selected because of the lower cost (~50% less) and its mechanical characteristics. The weight of only 1.5kg, the housing overall dimension of 100×100×100mm and the possibility to remove all the mechanical interface in front of the camera to directly access to the detector plane made the Xeva the most suited camera to be easily integrated into the opto-mechanics of the TCs. In table 2 a summary of the declared specifications and performance are shown.

XEVA-FPA-320 by XenICs		
Array type and format	InGaAs 320×256 pixels 30 μm pitch	
Maximum Frame rate	60 Hz full frame; 1 KHz 8×32pixels window	
Exposure time	1 μs to 5 min	
Mean Quantum Efficiency	75%	
Dark Current at 15 $^{\circ}\text{C}$	12500 e ⁻ /s/pix	
Operating temperature range	-40 to +70 $^{\circ}\text{C}$	
Detector cooling	1 thermoelectric stadium (liquid cooled)	
	LOW GAIN	HIGH GAIN
Saturation Charge	3750000 e ⁻	187500e ⁻
Readout Noise at 15 $^{\circ}\text{C}$	1099 e ⁻	114 e ⁻

Table 2 Specification and declared performance of the Xeva camera by Xenics

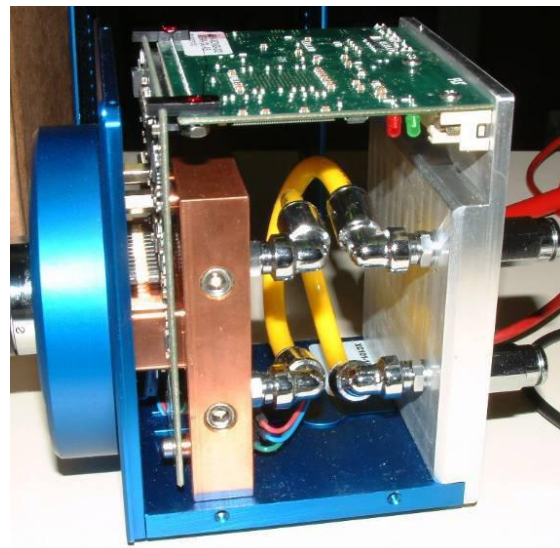


Figure 5 Close view of the Xeva camera with the cover removed.

The Xeva camera is shown in figure 5. In figure 2 only the hoses and cables which connect the camera to the cooling circuit and to the support electronics are visible at the top of the central cylinder since the IR camera is protected inside the cover. Two extenders, one for the USB connection and one for the Camera Link (CL) connection, are used to connect the camera to the control computer (a PC) located in a temperature controlled ambient several tens of meters way from the TC. The software library provided with the camera uses the USB to control the camera and the CL to enable the fast data download needed to reach the high frame rate required. The CL extender is the model PHOX-BM-00250 by PHRONTIER^{**} with a custom modification to meet the working temperature constrains while the USB extender is the model USB X-TENDER by Black Box^{††}. Both extenders are actually composed by two units: one is placed close to the PC and one close the camera. The two units are interconnected by means of a fibre optic pair (CL extender) or by a CAT 5 cable (USB extender). The units close to the IR camera are mounted on the chilling plate visible in figure 2.

As described in the previous paragraphs two linear stages and two motor units were used to remotely control the optical configuration of the TC. Four compact single axis controllers model C-862 Mercury, by PI, have been used to drive the

[‡] XenICs nv, Ambachtenlaan 44, B-3001 Leuven, BELGIUM

[§] FLIR Systems Inc., 27700A SW Parkway Ave, Wilsonville OR 97070, USA

^{**} PHRONTIER Technologies, 2211 Hacienda Blvd, Hacienda Heights CA 91745, USA

^{††} Black Box Corporation, 1000 Park Drive, Lawrence PA 15055-1018, USA

four units. The controllers are mounted on the chilling plate and are connected to the positioners by means of the four connectors visible in figure 2. In this way the central cylinder with the optical system can be quickly detached to easily handle it during installations at the telescope and in the laboratory.

Since the lenses L2 and L3 and the pupil stops move on the same space volume, an anti-collision system has been implemented to prevent any damage. The system is based on the real time monitoring of the Mercury controllers on the limit signals of the unit they drive. The anti-collision system has been implemented simply inserting on the limit sensor circuits a number of switches and/or relays raised d by the moveable parts of the TC.

The control software of the TCs has been based on the libraries provided by the IR camera and positioners suppliers. The basic aim was to provide a simple graphical interface to easily control the system configuration and to acquire data. In figure 6 the main control window is shown. The optical configuration can be easily changed using the buttons on the optical configuration bar. Another window allows to refine the position of each elements directly controlling each single positioner.

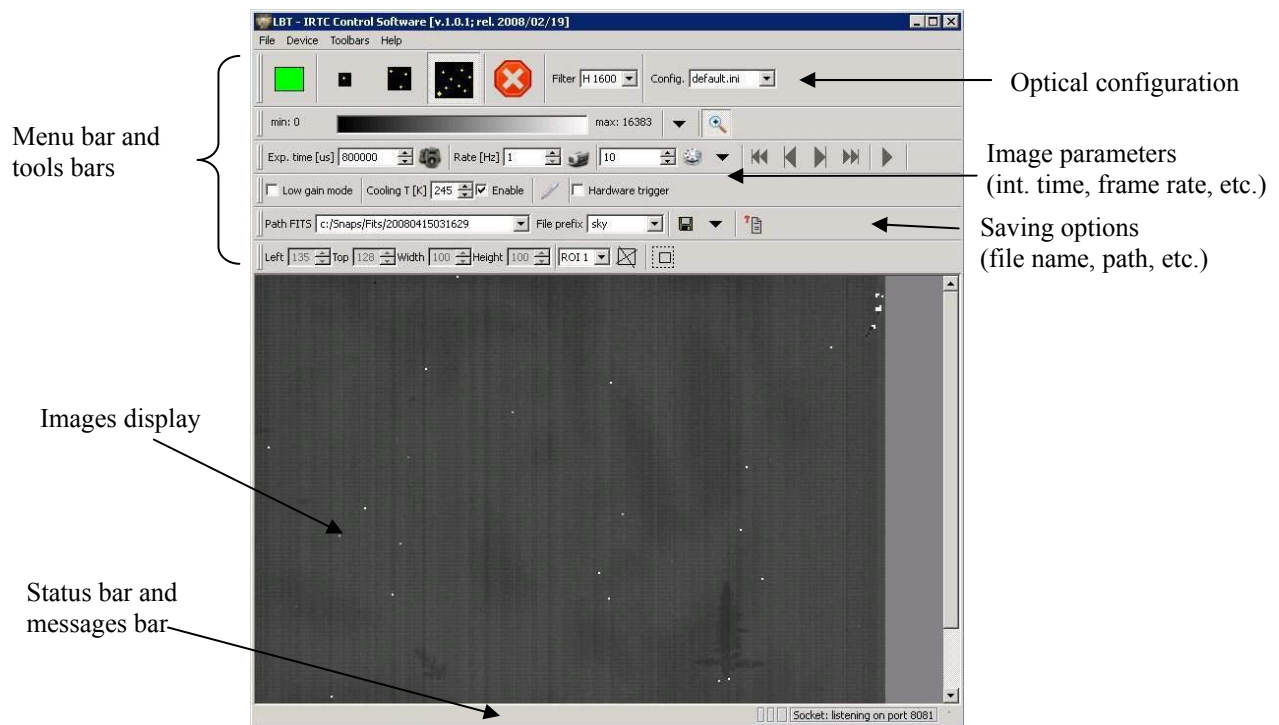


Figure 6 View of the control software main window.

The control software was also provided with a TCP/IP server to allow the user to remotely control a small set of basic functions (acquire an image, set the exposure time, control the parameters, etc.). In this way the functions that require to be executed hundreds of times during AO tests can be easily automated by means of a client application.

Finally a low level procedure is stored on the Mercury controller and it is automatically executed at the power up of the system to automatically initialize the positioners encoders.

3. INTEGRATION AND TESTS

All the components have been tested before the integration phase. In particular the IR cameras have been characterized to verify their efficiency and noise. By means of the photon transfer curve technique [6] the gains (G), i.e. the conversion factors electrons/ADU (Analog to Digital Units), have been measured. The signal variance, required to apply this technique, has been calculated for every single pixel over a set of 400 images rather than over an area of a single image. In this way we got rid of bright pixels, fixed pattern noise and uneven response quite evident on both detectors. Both cameras showed bad performance in low gain mode, probably due to the large capacitor used to store the signal charges in this mode: the mean value of G was ~ 300 e^- /ADU but the pixel to pixel variation reached the 100%. Conversely in high gain mode a value of G of 11 e^- /ADU with a pixel to pixel variation below 10% was measured for both cameras. The knowledge of G allowed to measure the quantum efficiency (QE) of the detectors using a calibrated photodiode as reference. In figure 7 the QE of the TC number 2 is shown. The QE of the other camera is similar.

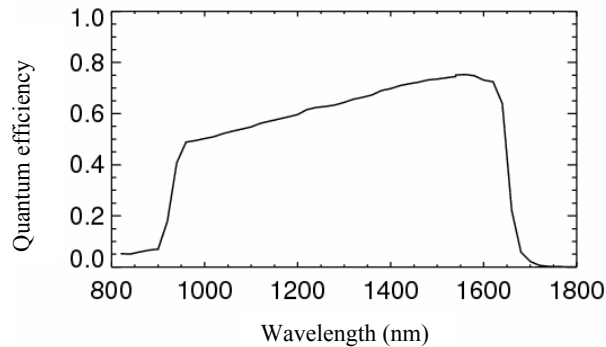


Figure 7 Quantum efficiency of the IR cameras mounted on the TC number 2. The QE of the other camera is similar.

The readout noise measured in low gain mode was about 2000 e^- /pixel for both cameras, which was roughly double with respect to the declared value. This was probably due to the ill defined value of G in this mode. In high gain mode readout noises of 150 e^- /pixel and 160 e^- /pixel have been measured for the two cameras.

The two main steps of the TCs integration were the electromechanical assembly and the optical assembly. During the first one all the electromechanical components in figure 4 were installed and wired as well as all the support electronics has been mounted on the chilling plate. Then they have been extensively tested paying a special attention to the anti-collision system and to the initialization procedure in order to prove their effectiveness and reliability. Also the control software has been tested to prove its ability to recognize and to recover, if possible, from collisions, missing hardware and unexpected events in general.



Figure 8 View of the opto-mechanics of the TC number 2.

The optical integration started with the definition of the optical axis with respect to the inner flange by means of an alignment mirror designed and machined to be precisely mounted at the centre of the flange. An hole in the centre of the mirror allowed do define the optical axis with a visible laser. The mechanics previously integrate was thus mounted on the flange and aligned by means of the adjustments on the interface. Finally the lenses have been mounted and their alignment has been checked moving the lenses L2 and L3 back and forth. An alignment precision of about one pixel has been obtained. In figure 8 a close view of the opto-mechanics of the TC number 2 is shown.

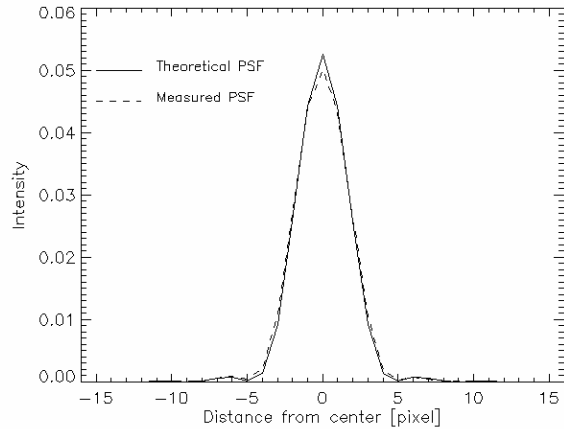
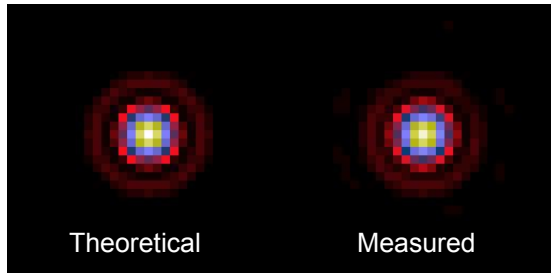


Figure 9 TC number 2: measured PSF in H band for the 3" FoV configuration. The measured PSF for the TC number 1 is similar.

An optical fibre with a core diameter of 9 μ m has been placed on the nominal entrance plane of the TCs (the telescope focal plane) and has been used to define the optical configurations and to test the optical quality of the system. Since an infinite number of configurations can be found adjusting L2 and L3 but just the three with the required pixel scale are optimized for the optical quality, the three optimal configurations have been found measuring the Sthrel ratio for a number of configurations obtained adjusting the lenses around their nominal positions. For the 30" FoV configuration the FWHM of the PSF has been measured instead of the Sthrel ratio.

In figure 9 the PSF measured for the TC number 2 in H band in the 3" FoV configuration is shown. In table 3 the measured performance in H band are summarized. The result for the TC number 1 are similar.

CONFIGURATION (FOV)	H BAND PSF QUALITY	
	<i>Measured</i>	<i>Reference (optical design)</i>
10 mas/pixel (3" FoV)	On axis SR 0.96 (FWHM 3.90 pixel)	On axis SR 0.97 (FWHM 3.84 pixel)
20 mas/pixel (6" FoV)	On axis SR 0.87 (FWHM 2.12 pixel) 3" off axis FWHM 2.13 pixel	On axis SR 0.96
100 mas/pixel (30" FoV)	On axis 80% EE in $\sim 2 \times 2$ pixel (FWHM 1.2 pixel) 4.2" off axis FWHM 1.2 pixel 8.4" off axis FWHM 1.2 pixel	On axis 80% EE in $\sim 2 \times 2$ pixel

Table 3 TC number 2: summary of the measured PSF quality in H band. The measurements for the TC number 1 are similar.

4. ON SKY PERFORMANCE

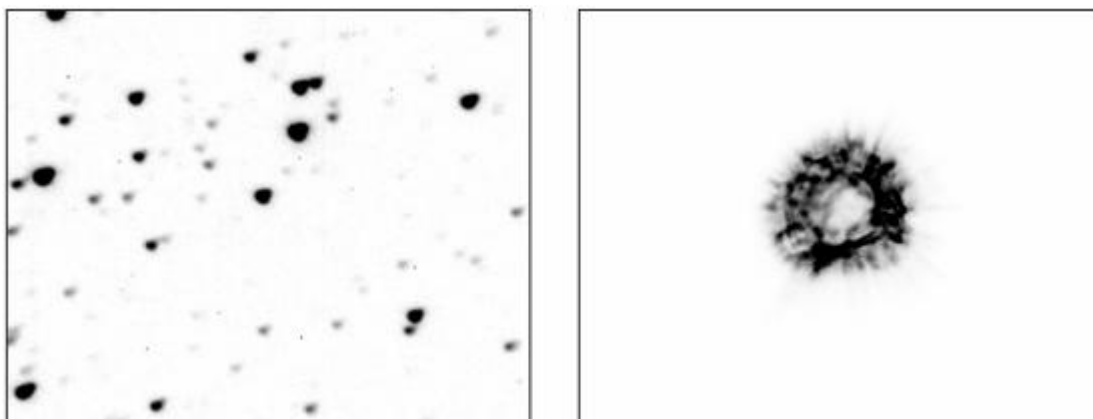


Figure 10 First light images of the TC number 2. An image of M13 is shown on the left and an out-of-focus image of a bright star in M5 is shown on the right.

In figure 10 two images obtained during the TC first light on sky are shown. Both are obtained in H band with the 30" FoV configuration. Both images are obtained adding 30 frames for a total exposure time of 30 seconds. The measured FWHM of the stars on the M13 image is about 0.55" even if the telescope collimation was not refined yet since these were the very first images on sky. The out of focus image of the bright star in M5 is an example of the images used to refine the telescope collimation table by means of curvature sensing techniques.

5. CONCLUSIONS

The optical performance measured in the laboratory and confirmed by the first seeing limited images on sky show that the achieved optical quality of the TCs fulfil the requirements. Moreover the absence of major issues during the installations in the laboratory (Arcetri) and on the mountain (LBT) as well as during the first months of operation, in particular for the one dedicated to the laboratory tests in Arcetri, confirms the reliability of the TCs. Finally the flexibility of the system has been proven to be useful on both laboratory and on sky activities.

The short realization time of about one year and the moderate cost (about 200K€ for the hardware and about 100K€ for manpower, shipping and travel) can be considered two other major goals achieved by the project.

6. ACKNOWLEDGMENTS

The TCs team would like to thank the directors of the institutes involved in the project for the constant support: Flavio Fusi Pecci (INAF – Osservatorio Astronomico di Bologna), Giorgio Palumbo (Università di Bologna, Dipartimento di Astronomia) and Hans-Walter Rix (Max-Planck-Institut für Astronomie, Heidelberg). The team would also like to thank Bruno Marano, Piero Salinari, Paolo Vettolani at INAF, Ray Bertram, Joar Brynnel, Richard Green, John Hill at LBTO, Wolfgang Gaessler, Lars Mohr at MPIA for the suggestions and the support during all phases of the project.

Finally a special thank to Jose Borelli (MPIA) for the kind collaboration during the development of the instrument simulator software.

REFERENCES

- [1] Hill, J., M., Salinari, P., "Large Binocular Telescope project", Proc. SPIE 3352, 23-33 (1998)
- [2] A. Riccardi, G. Brusa, P. Salinari, S. Busoni, O. Lardiè, P. Ranfagni, D. Gallieni, R. Biasi, M. Andrighettoni, S. Miller, and P. Mantegazza, "Adaptive secondary mirrors for the Large Binocular Telescope," in *Astronomical Adaptive Optics Systems and Applications*, R. K. Tyson and M. Lloyd-Hart, Eds., Proc. SPIE 5169, 159–168 (2003)
- [3] Giallongo, E., Ragazzoni, R., Grazian, A., Baruffolo, A., Beccari, G., de Santis, C., Diolaiti, E., di Paola, A., Farinato, J., Fontana, A., Gallozzi, S., Gasparo, F., Gentile, G., Green, R., Hill, J., Kuhn, O., Pasian, F., Pedichini,

- F., Radovich, M., Salinari, P., Smareglia, R., Speziali, R., Testa, V., Thompson, D., Vernet E., Wagner, R., M., “The performance of the blue prime focus Large Binocular Camera at the Large Binocular Telescope”, *Astronomy & Astrophysics* 482, 349-357 (2008)
- [4] Storm, J., Seifert, W., Bauer, S.-M., Dionies, F., Hanschur, U., Hill, J., M., Moestl, G., Salinari, P., Varava, W., Zinnecker, H., "Wavefront sensing and guiding units for the Large Binocular Telescope", *Proc. SPIE* 4007, 461-469 (2000)
- [5] Mandel, H., Appenzeller, I., Bomans, D., Eisenhauer, F., Grimm, B., Herbst, T., M., Hofmann, R., Lehmitz, M., Lemke, R., Lehnert, M., Lenzen, R., Luks, T., Mohr, R., Seifert, W., Thatte, N., A., Weiser, P., Xu, W., "LUCIFER: a NIR spectrograph and imager for the LBT", *Proc. SPIE* 4008, 767-777 (2000)
- [6] Janesick J., R., "Scientific Charge-Coupled devices", *SPIE Press Monograph*, Bellingham Washington, 101-130 (2001)